Journal of Applied Spectroscopy, Vol. 79, No. 5, November, 2012 (Russian Original Vol. 79, No. 5, September–October, 2012)

EFFECTIVE OPTICAL CONSTANTS OF COMPOSITE MATERIALS WITH AN ARBITRARY VOLUME CONCENTRATION OF NANOINCLUSIONS

A. N. Ponyavina,[a*] S. M. Kachan,[b] and E. E. Tselesh[a]

UDC 537.876.23+543.42:621.373

A new mixing rule for the effective dielectric constant of composite materials is formulated on the basis of a probabilistic approach for describing the structure of granular composite structures. The advantages of the proposed model become apparent for high concentrations of inclusions with optical constants that differ significantly from those of the matrix. The distinctive feature of this model compared to the Maxwell Garnett rule is symmetry of the computational formulas and their invariance with respect to the numbering order of the materials, as well as the possibility of describing the two-mode structure of the surface plasmon resonance absorption band in metal-dielectric nanocomposites with a high concentration of the metallic phase.

Keywords: *densely packed nanostructures, effective dielectric constant, surface plasmon resonance.*

Introduction. At present the most widespread method of describing the optical properties of ultradispersed composite systems is the effective medium approximation (EMA) [1–7]. With it, the effective dielectric constant ε_{eff} can be calculated using, for example, the Maxwell Garnett (MG) formula, the Bruggeman formula, or any of their numerous modifications, which are analyzed in some detail in [5]. However, the use of these approaches is limited by two circumstances. First, in principle, representing a dispersed medium as a quasiuniform medium and introducing effective optical parameters excludes the possibility of evaluating the scattering characteristics of this medium. Second, given the simplified assumptions regarding the topology of the medium, each of these models has a limited domain of applicability and cannot describe the entire set of experimental data. At the same time, the relative simplicity of the analytic expressions typical of these models can, in many cases, be a significant argument in choosing a method for the quasiquantitative description of experimental results. For this reason, it is useful to determine just how completely the best known EMA models are able to describe the major trends in the variation of the optical parameters of nanocomposites as their composition and microstructure are varied.

Thus, for example, it is known that the Bruggeman approximation for the effective dielectric constant applies to a two-component medium with a structure close to an ideal random mixture where it is impossible to make a clear separation between inclusions and the matrix. In contrast, the MG theory is for composites that contain distinct discrete inclusions, but it applicability is limited to low volume concentrations of the dispersed phase. Each of the theories has its pluses and minuses when compared with experiment. For example, surface plasmon resonance absorption (SPRA) bands in metal-dielectric nanocomposites can only be described by the MG theory, and the percolation threshold for their conductivity, only by the Bruggeman theory.

An attempt has been made to combine the advantages of these two theories by Sheng [6]. Although the resulting expressions for ε_{eff} are very cumbersome, they do describe the SPRA bands and the percolation conductivity threshold. Formulas for ε_{eff} that are much more convenient for calculations but have the same physical advantages as those of Sheng can be derived using the combined model (CM) of an effective medium described in this paper. This approach is most effective in the optical range of the spectrum, where the object of discussion is the effective optical characteristics of composites, such as the effective refractive index n_{eff} and absorption coefficient κ_{eff}.

[*]To whom correspondence should be addressed.

[a]B. I. Stepanov Institute of Physics, National Academy of Sciences of Belarus, 4 Nezavisimost' Ave., Minsk, 220072, Belarus; e-mail: ponyavin@imaph.bas-net.by; [b]Belarusian National Technical University, Minsk. Original article submitted December 14, 2011. Translated from Zhurnal Prikladnoi Spektroskopii, Vol. 79, No. 5, pp. 765–773, September–October, 2012.

 0021-9037/12/7905-0754

Computational Technique. Let us consider a two-component composite with a granular structure and comparable concentrations of the component phases, such that it is impossible to separate strictly the inclusion and the matrix phases. This kind of topology is realized, for example, in vacuum deposition technologies for creating granular coating with comparable concentrations of the constituents [7]. In this situation (in the range where the matrix undergoes an inversion) it is necessary to account for the finite probability of two different types of composite medium in localized parts of the composite: type 1 corresponds to the situation where grains of material 1 (with dielectric constant ε_1) are in a matrix of material 2 (with dielectric constant ε_2) and type 2, to the situation where the grains of material 2 are in a matrix of material 1. We denote the probabilities of realizing these events by w_1 and w_2. Then the effective dielectric constant averaged over the different realizations at some local point can be defined as

$$\varepsilon_{\text{eff}}^{\text{CM}} = (\varepsilon_{\text{eff}})_1 w_1 + (\varepsilon_{\text{eff}})_2 w_2 . \tag{1}$$

The $(\varepsilon_{\text{eff}})_i$ in Eq. (1) are found using the MG relations [1],

$$\frac{\varepsilon_{\text{eff}}^{\text{MG}} - \varepsilon_0}{\varepsilon_{\text{eff}}^{\text{MG}} + 2\varepsilon_0} = p_i \left(\frac{\varepsilon_i - \varepsilon_0}{\varepsilon_i + 2\varepsilon_0} \right).$$

After some elementary transformations, we obtain

$$(\varepsilon_{\text{eff}})_i = (\varepsilon_{\text{eff}}^{\text{MG}})_i = \frac{2\varepsilon_0 (\varepsilon_i - \varepsilon_0) p_i + \varepsilon_0 (\varepsilon_i + 2\varepsilon_0)}{(\varepsilon_i + 2\varepsilon_0) - (\varepsilon_i - \varepsilon_0) p_i}, \tag{2}$$

where $\varepsilon_i = \varepsilon_i' + i\varepsilon_i''$ is the complex dielectric constant of the grain material and $\varepsilon_0 = \varepsilon_0' + i\varepsilon_0''$ is that of the matrix material into which the grains are incorporated.

To determine the probabilities w_1 and w_2 in Eq. (1) as functions of the relative volume concentrations of the components of the composite, we use arguments similar to those in [6]. Let us consider a spherical region inside the composite where a fraction p_1 of the volume is occupied by molecules of species 1, while the remainder of the volume is occupied by $p_2 = 1 - p_1$ molecules of species 2. Here p_1 and p_2 are the macroscopic volume concentrations of substances 1 and 2. As a result of diffusion or the coalescence of the molecules, two situations are possible: substance 1 forms a grain and substance 2, a coating, or substance 2 forms a grain and substance 1 a coating. The relative probabilities of these two cases can be estimated by counting the number of equally probable final configurations corresponding to different positions of the grains within the region being considered. We assume that the grains formed by diffusion or coalescence are spherical in shape. Then, for the event corresponding to formation of a grain of substance 1 in the region under consideration the number of configurations is proportional to $\nu_1 = (1 - p_1^{1/3})^3$, i.e., to the free volume accessible for the center of a grain of this material. For the same reasons, the number of configurations for the alternative situation involving formation of a grain of substance 2 is proportional to $\nu_2 = [1 - (1 - p_1)^{1/3}]^3$. Thus, for any values of p_1 and p_2, the relative probability of the first case is $w_1 = \nu_1/(\nu_1 + \nu_2)$ and that of the second, $w_2 = 1 - w_1 = \nu_2/(\nu_1 + \nu_2)$. Despite its simplicity, this approach can be used to describe the major experimentally observed behavior of the composite with changes in its topology as a functions of the concentrations p_1 and p_2, including within the region $p_1 = 0.35$–0.65 corresponding to the range of a structural transformation in which the matrix is inverted.

Then, according to the proposed CM, the final formula for the effective dielectric constant $\varepsilon_{\text{eff}}^{\text{CM}}$ is

$$\varepsilon_{\text{eff}}^{\text{CM}} = w_1 \frac{2\varepsilon_2 (\varepsilon_1 - \varepsilon_2) p_1 + \varepsilon_2 (\varepsilon_1 + 2\varepsilon_2)}{(\varepsilon_1 + 2\varepsilon_2) - (\varepsilon_1 - \varepsilon_2) p_1} + w_2 \frac{2\varepsilon_1 (\varepsilon_2 - \varepsilon_1)(1 - p_1) + \varepsilon_1 (\varepsilon_2 + 2\varepsilon_1)}{(\varepsilon_2 + 2\varepsilon_1) - (\varepsilon_2 - \varepsilon_1)(1 - p_1)}, \tag{3}$$

where $w_1 = (1 - p_1^{1/3})^3/[(1 - p_1^{1/3})^3 + (1 - p_2^{1/3})^3]$ and $w_2 = (1 - p_2^{1/3})^3/[(1 - p_1^{1/3})^3 + (1 - p_2^{1/3})^3]$.

Note that, for $p_1 = 0$, $\varepsilon_{\text{eff}}^{\text{CM}} = \varepsilon_2$, while for $p_1 = 0$, $\varepsilon_{\text{eff}}^{\text{CM}} = \varepsilon_1$. In addition, as $p_1 \to 0$, $\varepsilon_{\text{eff}}^{\text{CM}} \to (\varepsilon_{\text{eff}}^{\text{MG}})_1$; $p_1 \to 1$ $\varepsilon_{\text{eff}}^{\text{CM}} \to (\varepsilon_{\text{eff}}^{\text{MG}})_2$. Equation (3) can also be used to obtain the effective complex refractive index of the composite, $m_{\text{eff}} = n_{\text{eff}} - i\kappa_{\text{eff}}$, which is related to the effective complex dielectric constant by the well known formula $\varepsilon_{\text{eff}} = m_{\text{eff}}^2$. Hence, $\varepsilon_{\text{eff}}'(\lambda) = n_{\text{eff}}^2 - \kappa_{\text{eff}}^2$, $\varepsilon_{\text{eff}}''(\lambda) = 2n_{\text{eff}}\kappa_{\text{eff}}$.

In order to analyze the behavior when the features of closely packed media are included in the CM for the effective medium, we have studied the effect of the optical constants of the materials of the particles and matrix, as well as their relative concentrations on $\Delta = \varepsilon_{\text{eff}}^{\text{CM}} - \varepsilon_{\text{eff}}^{\text{MG}}$, the difference in the effective dielectric constants calculated using Eq. (3) and the MG rule. It was found analytically that the derivative of Δ with respect to ε_1' is characterized by four roots, two of which coincide and are degenerate. The degenerate roots correspond to $\varepsilon_1' = \varepsilon_2'$ and $\varepsilon_1'' = \varepsilon_2''$, i.e., to the case of a homogeneous medium. The two nondegenerate roots set the conditions for realizing two extrema of the function Δ, of which the maximum Δ can be discovered by analyzing the sign of the second derivative of this function. Thus, we can establish the range of parameters corresponding to the maximum differences between the two models for the effective medium.

For example, in the case of a real ε_2, the maximum of Δ corresponds to the condition

$$\varepsilon_1 = G/\varepsilon_2 ,$$

where

$$G = F_1/F_2,\ F_1 = 8(-1 + (1-p)^{1/3})^3\ (-1+p)\ p(-4+2p) - \sqrt{f}\ )\ (\sqrt{f}\, f_1 + f_2),$$

$$F_2 = 3(1 - 3(1-p)^{1/3} + 3(1-p)^{2/3} - 3p^{1/3} + 3p^{2/3})\ (3-p) + \sqrt{f}\ )^3\ (-p + \sqrt{f}\ )^3,\ f = 7 + (-4+p)\ p,$$

$$f_1 = 34 - 41p + 18p^2 - 3p^3,\ f_2 = 91 - 136p + 82p^2 - 24p^3 + 3p^4.$$

These equations show that the peak of Δ for a fixed volume concentration occurs when Im $\varepsilon_1 = 0$ and shifts to smaller Re ε_1 with increasing ε_2. The unwieldiness of these formulas makes further analytic study difficult. Thus, in order to estimate the dependence of Δ on the optical-structural parameters of the composite, we have done some illustrative calculations over a wide range of the parameters ε_i and p_i.

Figure 1a shows the dependence of Δ on the real part of the dielectric constant of the nanoparticles ε_1' for the case in which the materials of both the nanoparticles and the matrix are nonabsorbing ($\varepsilon_1'' = \varepsilon_2'' = 0$). Then the effective dielectric constant of the composite also has no imaginary part. The calculations were done for two volume concentrations of the nanoparticles in the composite (in the following we use the notation $p \equiv p_1$). The real part of the dielectric constant of the matrix was taken to be $\varepsilon_2' = 1(0.5)4.5$. It can be seen that for positive ε_1', the function $\Delta(\varepsilon_1')$ changes sign. Here the differences between $\varepsilon_{\text{eff}}^{\text{CM}}$ and $\varepsilon_{\text{eff}}^{\text{MG}}$ are most noticeable when the concentrations of the nanoparticle and matrix materials are similar ($p = 0.65$) and ε_1' and ε_2' differ substantially.

For the case where only the matrix material is nonabsorbing ($\varepsilon_2'' = 0$), Fig. 1b and c show the real (Δ_{Re}) and imaginary (Δ_{Im}) parts of Δ on the real part of the dielectric constant of the nanoparticles, ε_1'. The imaginary part of the dielectric constant of the nanoparticles was taken to be $\varepsilon_1'' = 0.5$, 1.0, 2.0. In this case, also, $\Delta_{\text{Re}}(\varepsilon_1')$ and $\Delta_{\text{Im}}(\varepsilon_1')$ change sign. Calculations were also done for two volume concentrations of the nanoparticles in the composite and show the same increase in the differences for $p = 0.65$ compared to $p = 0.90$. It is interesting that the increase in the imaginary part of the dielectric constant of the nanoparticles (ε_2'') has the opposite effect on Δ_{Re} and Δ_{Im}, with a decrease in Δ_{Re} and an increase in Δ_{Im} for fixed ε_1'.

The set of data shown in Fig. 1 confirms that, for transparent matrices, Δ_{Re} increases monotonically as the real part of the dielectric constant of the nanoparticles is increased and/or the imaginary part is decreased. On the other hand, Δ_{Im} increases monotonically when both the real or the imaginary parts of the dielectric constant of the nanoparticles are increased. For nontransparent matrices, these dependences (for both Δ_{Re} and Δ_{Im}) are nonmonotonic.

Figures 2 and 3 show the differences of the effective dielectric constants calculated using Eq. (3) and using the MG approximation as functions of the concentration p of the dispersed phase. These calculations were done with a step size $p = 0.01$ for real compositions whose components are characterized by a spread in the refractive index [8, 9] and the calculations have been done at characteristic wavelengths. For example, for Ag/SiO_2 composites, the chosen wavelengths are $\lambda = 0.65$ and 0.50 μm, which lie near the SPRA and the corresponding regions of negative ε_1'. For $\lambda = 0.65$ μm the dielectric constants of the components of the composite are given by $\varepsilon_{\text{Ag}} = -17.509 - i0.565$ and $\varepsilon_{\text{SiO}_2} = 2.391$, and for $\lambda = 0.5$ μm, by $\varepsilon_{\text{Ag}} = -8.234 - i0.287$ and $\varepsilon_{\text{SiO}_2} = 2.413$. It is interesting to note that in this frequency range for Ag/SiO_2 composite, Δ depends nonmonotonically on the concentration, while Δ_{Re} changes

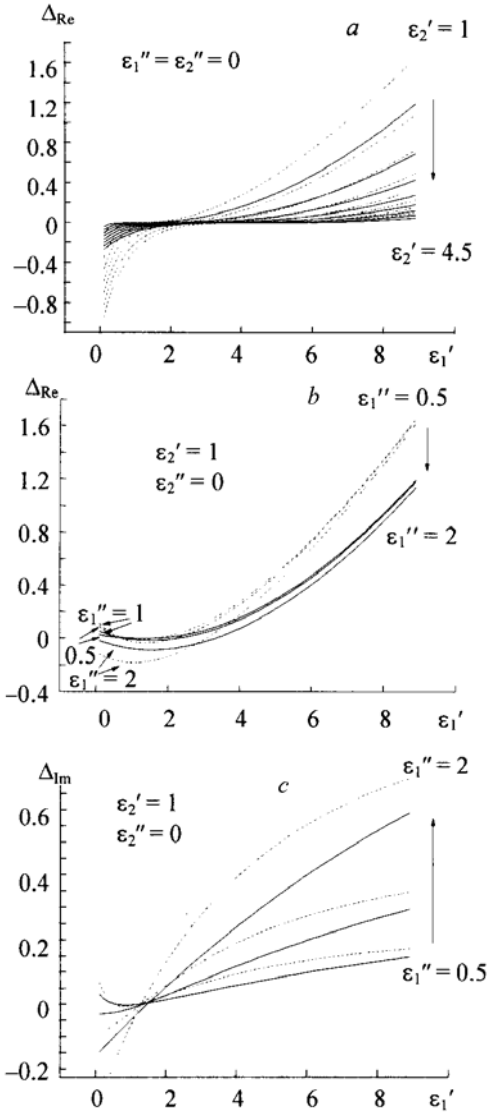

Fig. 1. The differences between the effective dielectric constants calculated using Eq. (3) and using the Maxwell Garnett approximation as functions of the optical constants of the particle and matrix materials; p = 0.90 (smooth curves) and 0.65 (dashed): (a) $\varepsilon_1'' = \varepsilon_2'' = 0$, (b) and (c) $\varepsilon_2'' = 0$.

sign. The differences between the models are insignificant for concentrations $p < 0.2$ and become quite substantial for p = 0.2–0.8. In all these cases the greatest differences for Δ_{Re} occur for nanoparticle concentrations near p = 0.65.

The dependence of Δ_{Im} on the concentration of metallic nanoparticles is characterized by a minimum with position and magnitude determined by the detuning from the frequency of the localized SPRA. Especially large deviations can be observed for Ag/SiO_2 composites and λ = 0.65 μm. This is evidently related to the closeness of this wavelength to the location of the peak of the SPRA band for concentrations p = 0.65 of silver nanoparticles in silica. We emphasize that these features of Δ are typical of nanocomposites for which the Froehlich condition $\varepsilon_{1(2)}(\omega) = -2\varepsilon_{2(1)}(\omega)$ [10] holds within some spectral region, e.g., metal-dielectric nanocomposites in the visible. The fact that a localized SPRA band of these composites appears in the spectrum near the Froehlich frequencies is reflected in the resonant character of the variation in the imaginary part of ε_{eff}, which is intrinsic both the CM and to the MG model [5–7].

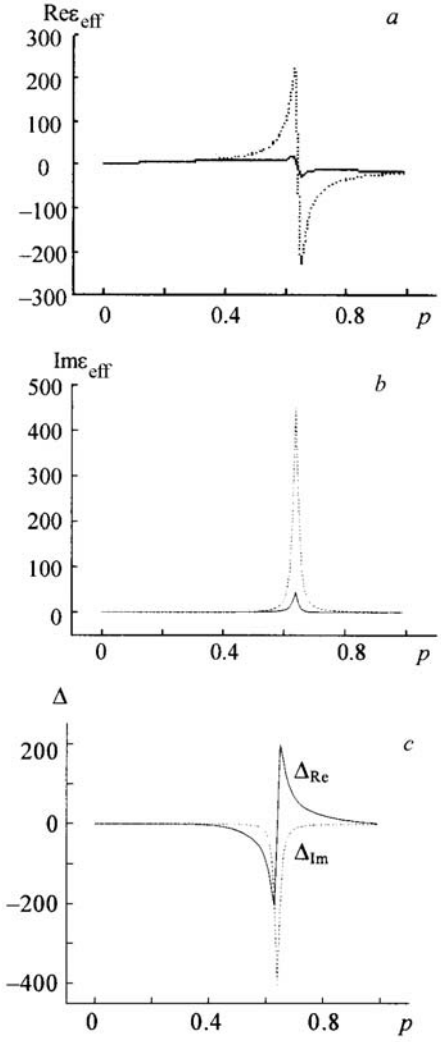

Fig. 2. The effective dielectric constants calculated using Eq. (3) (smooth curves) and using the Maxwell Garnett approximation (dashed curves) (a, b) and their difference (c) as functions of the concentration of the dispersed phase for Ag/SiO_2 composite: $\lambda = 0.65$ μm, $\varepsilon_{Ag} = -17.509 - i0.565$, $\varepsilon_{SiO_2} = 2.391$.

Results and Discussion. An analysis of Eqs. (2) and (3) shows that the differences from the dielectric constant of the composite medium calculated by the MG formulas are greatest when there is a substantial concentration of inclusions, and also for high values of the dielectric constant or in the spectral regions of the surface resonances. This is a reflection of the indirect accounting for the variation in the characteristics of the local field as the topology of the medium changes with changing concentration in the proposed CM. The concentration sensitivity of the local field and, therefore, of the difference in the complex effective refractive index ($n_{eff} - i\kappa_{eff}$) calculated by the CM will obviously increase when the optical contrast of the inclusions is greater.

An intuitive confirmation of this point can be obtained by, for example, comparing the real and imaginary parts of the complex effective refractive index calculated using the MG formula and Eq. (3) (Figs. 4 and 5). These calculations were done for porous materials (porous quartz and porous silicon), which are widespread in nature and are used in practical applications. The refractive index of silicon in the visible is characterized by strong dispersion and ranges over $n \approx 3$–5. The refractive index of quartz in the same spectral region is roughly constant ($n \approx 1.45$).

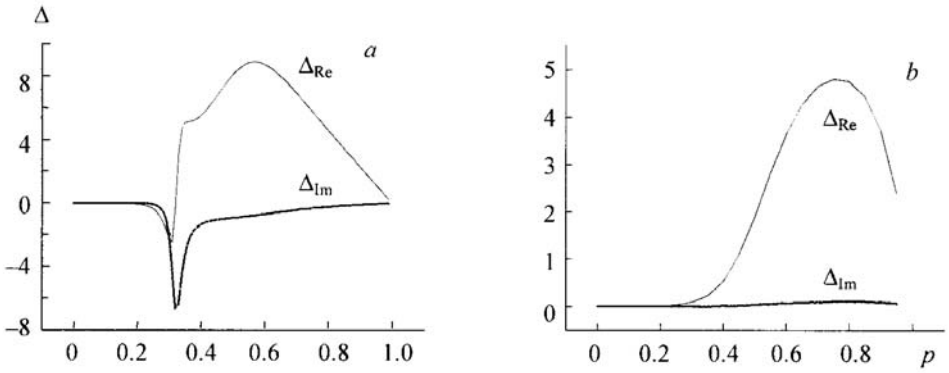

Fig. 3. The differences between the effective dielectric constants calculated using Eq. (3) and using the Maxwell Garnett approximation as functions of the concentration of the dispersed phase: (a) for Ag/SiO_2 composite, $\lambda = 0.5$ μm, $\varepsilon_{Ag} = -8.234 - i0.287$, $\varepsilon_{SiO_2} = 2.413$; (b) for porous silicon, $\lambda = 0.65$ μm, $\varepsilon_{Si} = 14.831 - i0.126$.

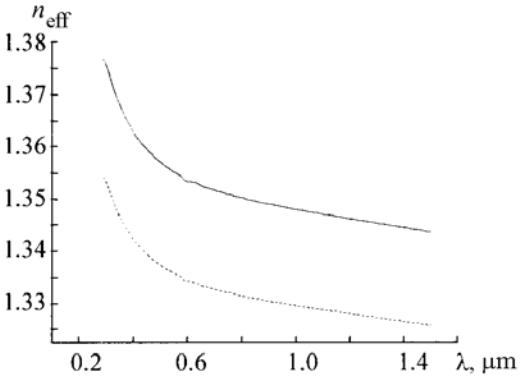

Fig. 4. Spectral variation of the real part of the effective dielectric constant calculated using Eq. (3) (smooth curve) and using the Maxwell Garnett approximation (dotted curve) for porous silica with a volume fraction of SiO_2 of $p = 0.65$.

A comparison of Fig. 4 with Fig. 5a and a′, shows that for the SiO_2—air system the difference between n_{eff}^{CM} and n_{eff}^{MG} is 1%, while for Si–air, this difference can approach 100%.

Even larger differences in the calculated n_{eff} and κ_{eff} occur for resonant systems, e.g., for metal-dielectric nanocomposites, which have SPRA in the visible. Thus, Fig. 6 shows some numerical calculations for silver nanospheres in a silicate matrix.

Figure 6a and b shows that for low concentrations of metallic nanoparticles (up to $p = 0.3$), the complex effective refractive indices calculated by both models are essentially the same over the entire visible range of the spectrum. There is a slight difference (10–15%) in a narrow region at $\lambda \approx 0.5$ μm, corresponding to the position of the SPRA for low concentrations of the metallic nanoparticles. At the same time, for $p = 0.65$ (Fig. 6a′ and b′), the results of these calculations are quite different, especially in the region of 0.6–0.7 μm, which corresponds to the location of the collective SPRA for these concentrations of the metallic nanoparticles. In this range of wavelengths and concentrations, there is a fourfold difference in n_{eff} and κ_{eff} as calculated using Eqs. (2) and (3). An analysis of Fig. 6 shows, therefore, that, for plasmon-resonance systems, the characteristics of the local field and the SPRA bands are extremely sensitive to the topology of the nanocomposite.

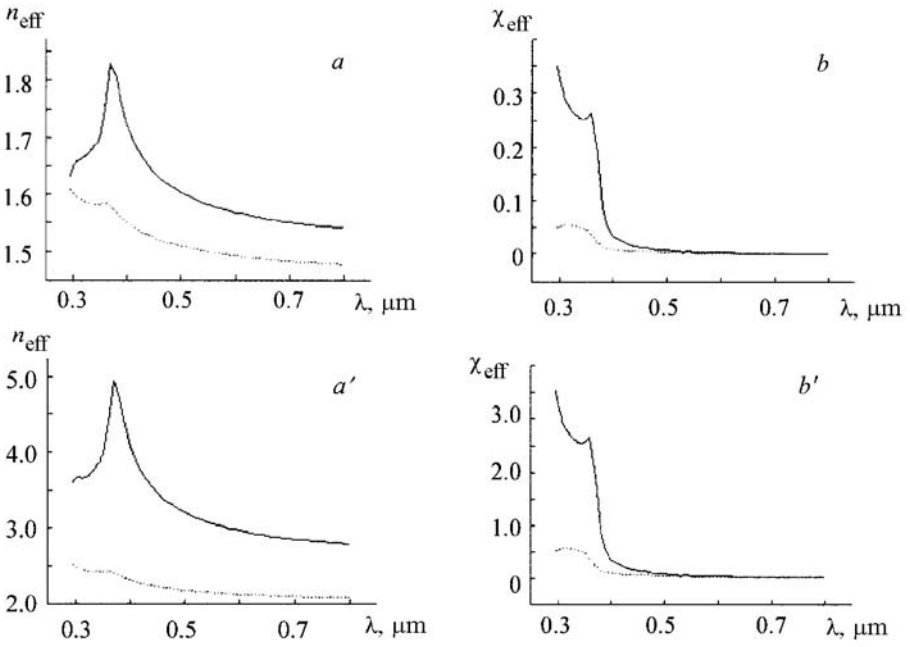

Fig. 5. Spectral variations of the real (a, a′) and imaginary (b, b′) parts of the effective refractive index calculated using Eq. (3) (smooth curve) and using the Maxwell Garnett approximation (dotted curve) for porous silica with volume concentrations of Si, $p = 0.35$ (a, b) and $p = 0.65$ (a′, b′).

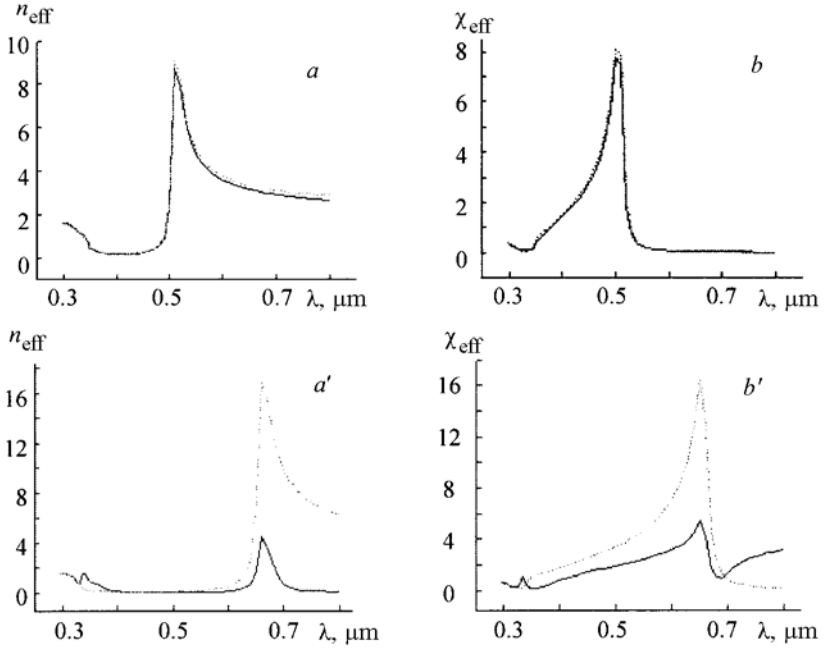

Fig. 6. Spectral variations of the real (a, a′) and imaginary (b, b′) parts of the effective refractive index calculated using Eq. (3) (smooth curve) and using the Maxwell Garnett approximation (dotted curve) for Ag/SiO_2 composite with volume concentrations of Ag of $p = 0.35$ (a, b) and $p = 0.65$ (a′, b′).

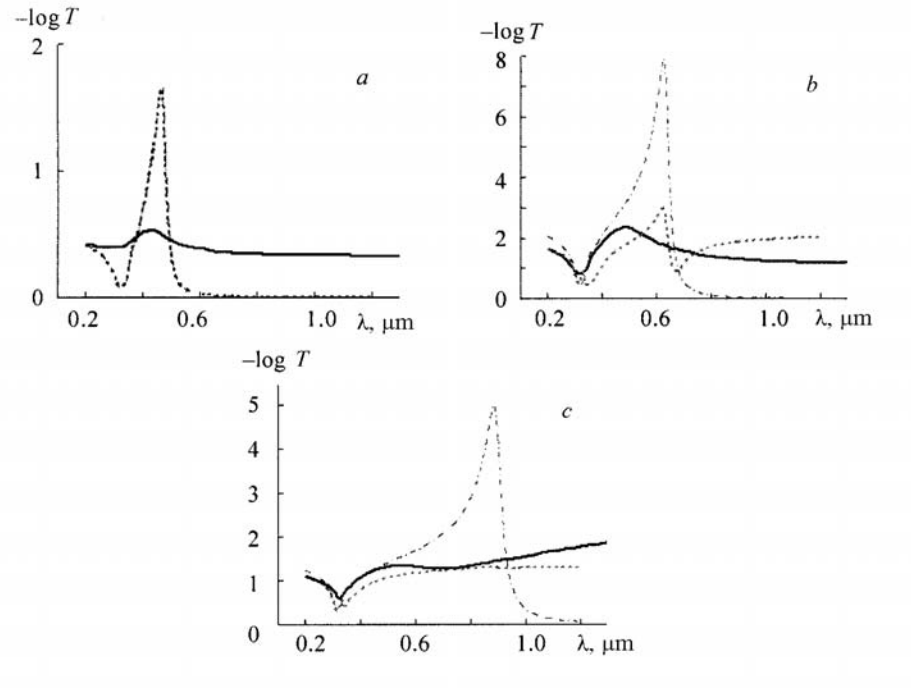

Fig. 7. Spectral dependences of the optical density of granular Ag/SiO_2 nanocomposite films of thickness L with a volume content of silver p obtained experimentally (smooth curves) and calculated using the combined model (dotted) and the Maxwell Garnett model (dot-dashed curve): (a) $p = 0.30$, $L = 32$ nm; (b) $p = 0.64$, $L = 82$ nm; (c) $p = 0.83$, $L = 41$ nm.

It is important to emphasize that calculations using the MG formulas for substantial concentrations of the metal in a composite will yield an optical density greatly in excess of that found in the region of an SPRA band [5, 6]. Thus, we can say that the tendency toward a decrease in κ_{eff}^{CM} relative to κ_{eff}^{MG} shown in Fig. 6 is suggests that it may be better to use the CM for calculating the optical density of plasmon-resonant composites with large amounts of a metallic phase.

This conclusion is confirmed by a direct comparison of the CM and MG model calculations with experiment. In the calculations the optical constants of silver from [8] were used and the dielectric constant of SiO_2 was assumed equal to 2.2 ($n = 1.4832$). The experimental data for Ag/SiO_2 nanocomposites were taken from [11]. For convenience in comparing the experimental and theoretical results, the experimental curves are normalized so they coincide with the calculations at short wavelengths. Figure 7 shows that, for low concentrations of silver nanoparticles embedded in an Ag/SiO_2 matrix ($p = 0.3$), the optical densities calculated using the CM and the MG model essentially coincide and exceed the experimental values in the SPRA region. This may be related to the strong broadening of the experimental SPRA owing to the polydispersivity of the real nanocomposite and the size dependence of the optical constants of the Ag nanoparticles. The advantages of the CM show up at medium concentrations of silver ($p = 0.64$), which correspond to the inversion zone for the matrix. The CM calculations for these values of p are very close to experiment, while the MG model yields values of the SPRA that are high by a factor of more than three. The advantages of the CM show up even more strongly near silver concentrations of $p = 0.83$, when inversion of the matrix is already complete and the composite consists of SiO_2 nanoparticles embedded in silver. At these concentrations the MG model still implies the existence of a strong silver SPRA, while the SPRA band of silver is almost entirely absent in the experiment and in the CM calculations.

One vital advantage of the proposed CM is that Eq. (3), as opposed to the MG formula, is symmetric and the result of a calculation with it is independent of the chosen order of enumerating the materials. For example, if the volume fraction of one of the materials (the metal) in the composite is 40%, while that of the other (the dielectric) is

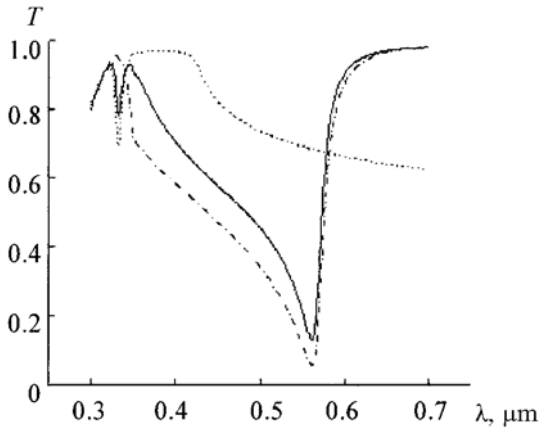

Fig. 8. Spectral dependence of the transmission coefficient $T = \exp(-4\pi\kappa_{eff}l/\lambda)$ of a composite Ag/SiO_2 film of thickness L = 10 nm with a volume concentration of Ag of p = 0.5: calculations using the combined model and Eq. (3) (smooth curve) ; using the Maxwell Garnett approximation assuming that the Ag particles are embedded in the SiO_2 matrix (dotted curve); and using the Maxwell Garnett approximation assuming that the SiO_2 fills the pores in a silver matrix.

60%, then Eq. (3) yields the same value of the effective dielectric constant of the composite whether we set $\varepsilon_{met} = \varepsilon_1$, p_1 = 0.4, $\varepsilon_{diel} = \varepsilon_2$, p_2 = 0.6 or $\varepsilon_{met} = \varepsilon_2$, p_2 = 0.4, $\varepsilon_{diel} = \varepsilon_1$, p_1 = 0.6. For this reason, when p = 0.5 (equal volume fractions of both materials) the calculation according to Eq. (3) is independent of which of the materials is regarded as an inclusion and which is the matrix. At the same time, the asymmetry of the MG formula yields a nonunique answer for p = 0.5: the effective dielectric constant of the composite medium and, therefore, its optical spectra turn out to depend on which of the materials is regarded as the inclusion and which, the matrix. This shows up most clearly in the calculated characteristics of plasmon-resonance nanocomposites (Fig. 8).

An analysis of Eq. (3) also yields another physically obvious result that does not follow from the MG formula. When there is a significant volume concentration of a metallic ultradispersed phase in a composite where both metallic nanoparticles surrounded by a dielectric matrix and dielectric "voids" surrounded by a quasicontinuous metallic phase are encountered, two types of surface modes can develop (see Fig. 6a′ and b′). First, there are the well studied plasmon resonances on metallic nanoparticles (in particular at $\lambda \approx 650$ nm) and, second, there are the less well known plasmon resonances on dielectric nanopores (dielectric inclusions) in the metal ($\lambda \approx 335$ nm). These two groups of plasmon resonances lie in different spectral regions. The first group corresponds to the condition $\varepsilon_1 = -2\varepsilon_2$ and the second, to $2\varepsilon_1 = -\varepsilon_2$ [10]. For the typical frequency dependence of the dielectric constant of the metal in the Drude model, the modes of the second group occur at higher frequencies than those of the first group. For real, even very monodispersed composites, the modes of both types are, of course, strongly broadened by collective interactions. Nevertheless, the large spectral interval between them suggests that, under favorable conditions, they can be resolved in experimental spectra. An SPRA band associated with resonance absorption on "voids" in a metal-dielectric composite has been observed experimentally [12], with a faint absorption band detected at short wavelengths ($\lambda \approx 350$ nm) in an analysis of the measured transmission and reflection spectra of a composite.

As noted above, the main subject of this paper is the concentration dependence of the optical properties of nanocomposite structures with different compositions. Nevertheless, it is useful to consider briefly the possibility using the CM to describe nonoptical characteristics of metal-dielectric composites, such as conductivity and percolation behavior that shows up at low frequencies. Figure 9 shows the dependences of the effective conductivity $\sigma_{eff} = (\omega/4\pi)\mathrm{Im}\,\varepsilon_{eff}$ of granular Ag/SiO_2 nanocomposite on the volume fraction of silver calculated using the MG model and the CM. For calculating the imaginary part of ε_{eff} at λ = 1.93 μm, the values ε''_{Ag} = 6.758 [9] and ε_{SiO_2} = 2.2 [8] were

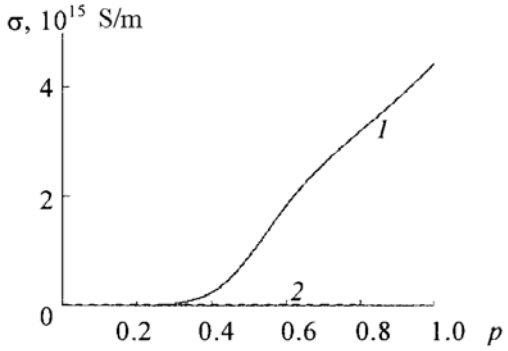

Fig. 9. Specific conductivity σ of granular Ag/SiO_2 composite as a function of the volume fraction of silver calculated using the combined model for the effective medium (*1*) and the Maxwell Garnett model (2); λ = 1.93 μm, ε''_{Ag} = 6.758, ε_{SiO_2} = 2.2.

used. The CM provides a qualitative description of the percolation properties of the metal-dielectric composite. For this case the effective conductivity of the composite increases quite rapidly for metal concentrations in the range p = 0.35–0.65, and as $p \to 1$ essentially approaches the conductivity of the bulk metal. Applying the MG model to the same object does not lead to a significant increase in the conductivity of the composite with increasing volume concentration of the metallic phase. We believe that these fundamental differences in the conductivity calculated with the MG model and the CM are related to the use of a probabilistic approach for describing the structure in the CM. Here, although the simplified approach used in the CM also neglects interactions between neighboring regions during grain formation, it can describe the structural transition regime responsible for percolation processes. Thus, it can easily be shown that for metal concentrations p = 0.35–0.65, the relative probability of detecting metal nanoparticles in the dielectric matrix $w_1 = (1 - p_1^{1/3})^3/[(1 - p_1^{1/3})^3 + (1 - p_2^{1/3})^3]$ drops sharply from 0.92 to 0.08, with the quantity $w_2 = 1 - w_1$ respectively increasing sharply (from 0.08 to 0.92). This is the reflection of the fact that the matrix has been inverted (from dielectric to metallic), which leads to a sharp rise in the effective conductivity of the metal-dielectric composite as the concentration of the metallic phase is raised over p = 0.35–0.65.

Conclusion. The use of a probabilistic approach for describing the structure of a granular composite makes it possible to formulate a mixing rule for the effective dielectric constant of composite materials that applies to arbitrary volume concentrations of the inclusions. For low inclusion concentrations, the combined model of an effective medium proposed here on the basis of this approach yields results that are essentially the same as calculations employing the Maxwell Garnett approximation. The advantages of using the new mixing rules (the combination model for an effective medium) show up at higher inclusion concentrations, where the optical characteristics are substantially different from those of the matrix. The definite advantages of the proposed model include symmetry of the computational formulas and the fact that the results are independent of the numerical ordering of the constituent materials, as well as the ability to describe the two-mode structure of surface plasmon resonance absorption in metal-dielectric nanocomposites with high concentrations of the metallic phase.

REFERENCES

1. J. C. Maxwell Garnett, *Philos. Trans. R. Soc. London. A,* **203**, 385–420 (1904).
2. D. A. G. Bruggeman, *Ann. Phys*., **24**, 636–679 (1935).
3. R. Ruppin, *Opt. Commun*., **182**, 273–279 (2000).
4. P. Chylek, V. Srivastava, R. G. Pinnick, and R. T. Wang. *Appl. Opt*., **27** (12), 1–9 (1988).
5. R. J. Gehr and R. W. Boyd, *Chem. Mater*, **8** 1807–1819 (1996).
6. Ping Sheng, *Phys. Rev. Lett*., **45** (1), 60–63 (1980).
7. B. Abeles, P. Sheng, M. D. Coutts, and Y. Arie, *Adv. Phys*., **24**, 407–415 (1975).

8. E. D. Palik, ed., Handbook of Optical Constants of Solids, Academic Press Inc., Orlando (1985).
9. P. B. Johnson and R. W. Christy, *Phys. Rev. B*, **12**, 4370–4379 (1972).
10. C. Bohren and D. Huffman, *Absorption and Scattering of Light by Small Particles* [Russian translation], Mir, Moscow (1986).
11. R. W. Cohen, G. D. Cody, M. D. Coutts, and B. Abeles, *Phys. Rev. B*, **8**, 3689–3701 (1973).
12. A. Da Silva, C. Andraud, J. Lafait, and A. Dakka, *J. Phys.: Condens. Matter*, **12**, 4125–4139 (2000).